

Article ID: 1001-0742(2000)02-0161-11

A three-dimensional model for the transportation of Fe and Mn in Arha Reservoir

CHEN Xiao-hong¹, Allan J Brimicombe²

(1. Department of Geography, Zhongshan University, Guangzhou 510275, China. E-mail: eescxh@zsu.edu.cn; 2. School of Surveying, University of East London, Longbridge Road, Dagenham, ESSEX RM8 2AS, United Kingdom)

Abstract: Coupling with a three-dimensional (3D) hydrodynamic model and a suspended solids model, a 3D model for the transport of Fe and Mn in Arha Reservoir, China, was developed. The 3D velocity fields for the flood season are computed to drive the 3D model of Fe and Mn in which the processes of advection, diffusion, redox, sorption, desorption, deposition, and re-suspension are included. The model has been calibrated by matching observed fluid, suspended solids, and total concentrations of Fe and Mn in the water column and in the sediment, successively. The model simulated both horizontal and vertical gradients of Fe and Mn in Arha Reservoir. It was found that Fe and especially Mn stratify in accordance with the stratification of DO during summer. The redox cycles across the water sediment interface has a principal role in the rise of Fe and Mn concentrations in the overlying water. It was also found that Fe and Mn loadings from the tributaries have a carryover effect on the water quality through a secondary contamination in the reservoir.

Key words: three dimensional model; Fe; Mn; transport; flow field; Arha Reservoir

CLC number: X1 **Document code:** A

Introduction

Arha Reservoir is located in the plateau region of Southwest China. This reservoir, with a volume of 44.5 million m³, was built in 1960 and is the main fresh water source for the city of Guiyang. It is plagued with water quality problems due to upstream mineral exploitation. About 2000 tons of suspended solids are transported into the reservoir by the tributaries each year. Some 770 tons of Fe and 50 tons of Mn enter the reservoir from the tributaries annually. Fe and Mn pollution in the reservoir has become a serious problem for the city water supply (Chen, 1997).

The redox cycles of Fe and Mn in lakes are well documented (e.g. Morgan, 1964; Robbins, 1975; Hoffmann, 1981; Davison, 1981; 1982) and taken as the basic mechanisms and kinetics of the Fe(II)-Fe(III) and Mn(IV)-Mn(II) redox couples (Sung, 1980; Pankow, 1981). Some researchers have placed their emphasis on the chemical reactions and kinetics of substances including Fe and Mn in aquatic environments (Stumm, 1985; 1987). However, the numerous factors which influence the spatial and temporal distribution of substances in lakes and reservoirs can be divided into two groups: the specific reactivity of the chemical substances considered and the characteristics of the physical environment. A more realistic model should describe the Fe and Mn concentrations on the basis of both the chemical properties and the physical characterization of the reservoir (Imboden, 1985). Several investigators have considered the distribution of Fe and especially Mn profiles (Calvert, 1972; Elderfield, 1976) and mathematical models which simulate the behavior of Fe and Mn have been developed (Michard, 1971; Burdige, 1983). With some notable exceptions

(Robbins, 1975; Davison, 1981) such work has concentrated on marine systems. The diversity of Fe and Mn distributions which exist in the water column of reservoirs has received particularly little attention (Davison, 1982). In recent years, some conceptual models for the removal of Fe and Mn (Coffey, 1993; Dortch, 1995) and the distribution of chemical substances in lakes (Imboden, 1985; Division, 1985) have been developed. These models are one dimensional formulae with the basic assumption of no significant horizontal gradients (vertical one dimensional model) or vertical gradients (depth averaged model) for the spatial distribution of a chemical substance in a lake. 3D mathematical modeling for Fe and Mn transportation in lakes and reservoirs are comparatively less frequent in the literature.

Vertical one dimensional models overcome the shortcomings of the one-and two-box models (Imboden, 1985) in consideration of the specific bottom topography of lakes and the interaction between the water column and sediments. In the case of Arha Reservoir, however, the spacial distributions of Fe and Mn have considerable differences between the upstream portion and the reservoir center with Fe and especially Mn being distributed in a qua-stratification (Chen, 1997). The transport of Fe and Mn in Arha Reservoir is therefore a 3D phenomenon.

The transport and the subsequent deposition of heavy metals in reservoirs are dominated by hydraulic processes with fluvial processes as the primary mechanism responsible for the transport of heavy metals in the water body (Foster, 1996). Both the hydrodynamic and the redox processes are important mechanisms for the transport of Fe and Mn in Arha Reservoir. In this paper, a 3D hydrodynamic model is set up to drive a 3D Fe and Mn transport model. In this way, the dynamics of redox, advection, diffusion, sorption and desorption, desorption and re-suspension for Fe and Mn in the reservoir can be considered. The paper focuses on the physical processes though the redox processes and the reaction of Fe and Mn in the sediment are described in the model. The distributions of Fe and Mn are computed for the flood season.

1 3D hydrodynamic model for Arha Reservoir

Arha Reservoir (Fig. 1) is of medium size with a surface area of 3.4 km², the average depth is 13m. There are 4 tributaries which provide the total inflow of 108.43 million m³ per year. The annual water supply is 65.7 million m³. The wind speed is low in the reservoir basin, and the water flow in the reservoir is dominated by inflow and water intake. The flow state varies in both horizontal and vertical directions due to the complicated reservoir topography.

Usually a reservoir can be considered to be a number of horizontal layers. Dividing the water body into K layers in depth and assuming vertical static pressure, the flow equations of continuity and momentum for the K th layer in the reservoir are:

$$\frac{\partial \eta}{\partial t} + \sum \left\{ \frac{\partial}{\partial x} (H_k u_k) + \frac{\partial}{\partial y} (H_k v_k) + \frac{\partial}{\partial z} (H_k w_k) \right\} = 0, \quad (1)$$

$$w_{k-1/2} = w_{k+1/2} - H_k \left(\frac{\partial u_k}{\partial x} + \frac{\partial v_k}{\partial y} \right), \quad (2)$$

$$\frac{\partial u_k}{\partial t} + u_k \frac{\partial u_k}{\partial x} + v_k \frac{\partial u_k}{\partial y} + w_k \frac{\partial u_k}{\partial z} = f v_k - g \frac{\partial \eta}{\partial x} + A_x \frac{\partial^2 u_k}{\partial x^2} + A_y \frac{\partial^2 u_k}{\partial y^2} + \frac{1}{\rho H_k} (\tau_{x, k-1/2} - \tau_{x, k+1/2}), \quad (3)$$

$$\frac{\partial v_k}{\partial t} + u_k \frac{\partial v_k}{\partial x} + v_k \frac{\partial v_k}{\partial y} + w_k \frac{\partial v_k}{\partial z} = -f u_k - g \frac{\partial \eta}{\partial y} + A_x \frac{\partial^2 v_k}{\partial x^2} + A_y \frac{\partial^2 v_k}{\partial y^2} +$$

$$\frac{1}{\rho H_k} (\tau_{y, k-1/2} - \tau_{y, k+1/2}), \quad (4)$$

in which η = water surface elevation, H_k = thickness of the K th layer, u_k, v_k = velocity components in x and y directions, respectively, f = Coriolis parameter, ρ = water density, A_x, A_y = turbulent viscosity coefficient components in x and y directions, respectively, $w_{k-1/2}, w_{k+1/2}$ = vertical velocity components on the upper and lower faces of the K th layer, respectively, $\tau_{x, k-1/2}, \tau_{x, k+1/2}$ = shear stress components on the upper and lower faces of the K th layer in x direction, respectively; $\tau_{y, k-1/2}, \tau_{y, k+1/2}$ = shear stress components in the upper and lower faces of the K th layer in y direction, respectively.

The shear stress in different layers is estimated by:

(1) bottom of the reservoir

$$\tau_{x, k+1/2} = \rho g u_k (u_k^2 + v_k^2)^{1/2} / c_1^2, \quad (5)$$

$$\tau_{y, k+1/2} = \rho g v_k (u_k^2 + v_k^2)^{1/2} / c_1^2. \quad (6)$$

(2) surface of the reservoir

$$\tau_{x, 1/2} = \rho_a c_a w_x (w_x^2 + w_y^2)^{1/2}, \quad (7)$$

$$\tau_{y, 1/2} = \rho_a c_a w_y (w_x^2 + w_y^2)^{1/2}. \quad (8)$$

(3) inner water body of the reservoir

$$\tau_{x, k-1/2} = \rho \gamma_1^2 (u_{k-1} - u_k) [(u_{k-1} - u_k)^2 + (v_{k-1} - v_k)^2]^{1/2}, \quad (9)$$

$$\tau_{y, k-1/2} = \rho \gamma_1^2 (v_{k-1} - v_k) [(u_{k-1} - u_k)^2 + (v_{k-1} - v_k)^2]^{1/2}. \quad (10)$$

In Equation (5)–(10), c_1 = Chezy coefficient, ρ_a = density of air, c_a = wind resistance coefficient, w_x, w_y = wind velocity components at the height of 10 meters above the reservoir surface in x and y directions respectively; γ_1 = resistance coefficient on the inner interfaces of the water body.

A staggered grid is used to discretize Equations(1)–(4) in both the horizontal and vertical directions of the computational domain. In the horizontal directions, a unit cell consist of a H -point and a ρ -point in the center, a u -point to its left, and a v -point to its bottom. The vertical velocities are computed on the upper and lower faces of a cell.

2 Model for the transport of Fe and Mn in the reservoir

The transport of Fe and Mn in reservoirs includes the processes of advection, diffusion, redox, adsorption, desorption, deposition and re-suspension. Advection is totally a hydraulic phenomenon. Diffusion includes molecular diffusion and turbulent diffusion. In the water column, turbulent diffusion mainly occurs, whilst in the sediment the amount of diffusion is very small. Both molecular diffusion and turbulent diffusion can be described by Fick's Law.

The redox process can be influenced by many factors such as pH, DO, temperature,

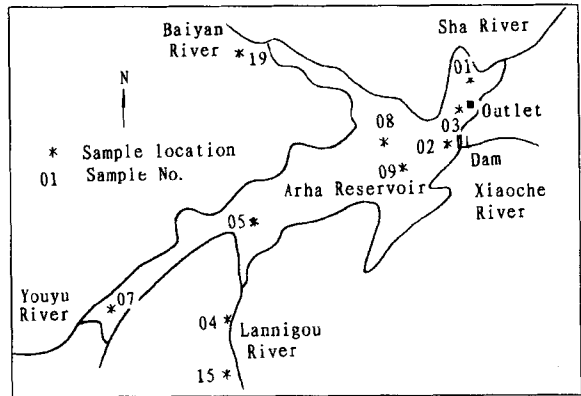


Fig.1 Plan of Arha Reservoir and location of samples

hydrodynamic behavior, physicochemical and biological processes (Gordon, 1989, Dortch, 1995). However, it is generally agreed that consistent relationships between the dynamic variables and these environmental factors cannot yet be described reliably (Shrestha, 1996). Morgan (Morgan, 1967) developed a reaction formula for the oxidation of dissolved manganese in which pH and DO are included. Rate constants are adjusted for temperature changes to standardize values. Hess *et al.* (Hess, 1989) used a similar model for Mn oxidation in the Chattahoochee River and pointed out that pH in natural water systems fluctuates diurnally and it is possible that the pH data may not be representative for modeling. The unsteady-state flow conditions which are not included in the model cause the poor model of dissolved Mn. The model does not consider the adsorption to the sediments and fails to predict particulate Mn concentrations accurately.

The purpose of this paper is to model the seasonal distributions of total Fe and Mn in the water column. The exchange or interaction between the dissolved and particulate Fe and Mn within the water column does not change the total Fe and Mn concentrations, and the oxidation in the sediments which increase the content of Fe and Mn in the permanent sediment layer does not influence the concentration in the overlying water either. Therefore, only the exchange between water (oxidation, deposition, and adsorption to the sediment) and sediment (reduction, desorption, and resuspension to the overlying water) need to be incorporated. The suspended solids within the water column, however, do need to be modeled because the processes of oxidation, deposition and resuspension are related to them.

Considering the two states of Fe or Mn in reservoir, the dissolved state C (mg/L) and the particulate state C_p (mg/L), the total concentration of Fe or Mn is

$$C_t = C + C_p. \quad (11)$$

Let C_{ts} be the total concentration in the surface sediment (mg/L) and S be the concentration of suspended solids (SS) in the water column (mg/L). By incorporating the processes of advection, diffusion, redox, adsorption/desorption, deposition, and resuspension of particulate Fe and Mn in the surface sediment, the 3D transport model for the concentration of total Fe or Mn in the water column and surface sediment can be described as:

$$\begin{aligned} \frac{\partial C_t}{\partial t} + u \frac{\partial C_t}{\partial x} + v \frac{\partial C_t}{\partial y} + w \frac{\partial C_t}{\partial z} = \frac{\partial}{\partial x} \left(E_x \frac{\partial C_t}{\partial x} \right) + \frac{\partial}{\partial y} \left(E_y \frac{\partial C_t}{\partial y} \right) + \frac{\partial}{\partial z} \left(E_z \frac{\partial C_t}{\partial z} \right) \\ - r_1 + r_2 + r_s - r_d + r_3 + J_c, \end{aligned} \quad (12)$$

$$\frac{\partial C_{ts}}{\partial t} + q_x \frac{\partial C_{ts}}{\partial x} + q_y \frac{\partial C_{ts}}{\partial y} + q_z \frac{\partial C_{ts}}{\partial z} = r_1 - r_2 + r_d - r_3 - r_s - r_p. \quad (13)$$

The transport of solids in the reservoir is described as:

$$\frac{\partial S}{\partial t} + u \frac{\partial S}{\partial x} + v \frac{\partial S}{\partial y} + w \frac{\partial S}{\partial z} = \frac{\partial}{\partial x} \left(D_x \frac{\partial S}{\partial x} \right) + \frac{\partial}{\partial y} \left(D_y \frac{\partial S}{\partial y} \right) + \frac{\partial}{\partial z} \left(D_z \frac{\partial S}{\partial z} \right) - v_s \frac{\partial S}{\partial z} + J_s, \quad (14)$$

in Equation (12)—(14), E_x , E_y , E_z = synthetic diffusion coefficients of Fe or Mn in x , y , z directions respectively in m^2/s , D_x , D_y , D_z = synthetic diffusion coefficients of SS in x , y and z directions respectively in m^2/s , r_1 , r_3 , r_d = variation rate of particulate concentration by oxidation, resuspension, and deposition, respectively, r_2 , r_s = variation rate of dissolved concentration by reduction and adsorption/desorption respectively, r_p = input rate of particles from surface sediment into permanent sediment layer, q_x , q_y , q_z = transport velocities of sediments in x , y and z directions respectively in m/s , v_s = settling velocity of particles (m/d), J_c = net inflow of total Fe or Mn concentration ($\text{mg}/(\text{L}\cdot\text{s})$), J_s = net input of particles ($\text{kg}/(\text{L}\cdot\text{s})$).

The kinetics of oxidation, reduction, resuspension, adsorption/desorption, and input of

particles into permanent sediment layer are assumed to be first-order reactions:

$$r_1 = k_1 f_d C_t, \quad (15)$$

$$r_2 = k_2 C_{ts}, \quad (16)$$

$$r_3 = \omega[(1 - f_s)C_{ts} - (1 - f_d)C_t], \quad (17)$$

$$r_s = s_2(C_{ts} - C_t), \quad (18)$$

$$r_p = k_3 C_{ts}, \quad (19)$$

where k_1 , k_2 = reaction rate constants (1/s), ω = resuspension coefficient (1/s), s_2 = desorption coefficient (1/s), k_3 = input coefficient of particles from surface sediment into permanent sediment layer (1/s), f_d , f_s = fraction of dissolved compound relative to total concentration in water column and surface sediment respectively, in which, f_d can be described

by

$$f_d = (1 + k_p S)^{-1}, \quad (20)$$

$$k_p = m/C, \quad (21)$$

where m = concentration on a solid basis [mg/kg(d), kg(d) = kg dry weight solids], k_p = partition coefficient [L/kg(d)]. It is assumed that f_s has a same form as f_d .

In Arha Reservoir, the saturation of DO in summer has a stable stratification (Fig. 2).

The variations of Fe and Mn in the reservoir are related to the saturation of DO and SO_4^{2-} to some extent, and the higher concentrations of the sulfide occur with 70%—90% saturation of DO (Table 1). The variations of Fe and Mn, however, do not have a consistent relationship to pH

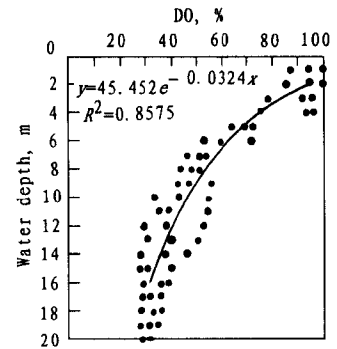


Fig.2 Vertical distribution of DO(%)

Table 1 Vertical distribution of pH, DO, Fe(II), Mn(II) and sulfide in reservoir center

Water depth, m	Temperature, °C	pH	DO, %	Fe, mg/L	Mn, mg/L	SO_4^{2-} , mg/L
1	24	7.8	84.5	0.33	0.01	239.0
2	23	7.99	78.3	0.53	0.14	230.5
3	22	7.85	76.7	0.30	0.06	240.0
4	22	7.70	74.5	0.29	0.02	248.6
5	22	7.81	72.7	0.28	0.03	235.7
6	22	7.76	75.7	0.27	0.02	240.0
7	21	7.54	51.1	0.48	0.50	253.0
8	21	6.96	51.1	0.75	0.31	253.0
9	21	7.47	58.2	0.30	0.34	253.0
10	21	7.65	57.3	0.26	0.05	242.6
11	20	6.85	56.7	0.35	0.19	247.5
12	20	6.71	54.0	0.67	0.46	246.1
13	20	6.68	53.4	0.28	0.35	248.6
14	20	6.62	48.5	1.05	0.69	272.0
15	20	6.51	43.0	0.44	1.07	270.2
16	19.5	7.22	42.0	0.50	0.98	278.0
17	18.5	7.32	32.1	0.31	1.50	282.3
18	17	7.48	36.2	0.34	2.10	263.3
19	166.6	7.45	33.3	0.31	2.30	269.4
20	15.5	7.51	32.1	0.33	2.60	260.7

in Arha Reservoir(Chen, 1997). Considering that sulfide in Arha Reservoir is related to saturation of DO, and that saturation of DO itself is influenced by many factors such as temperature, aerobic or anaerobic conditions, light conditions, and pH, it is easy to include saturation of DO directly into the redox reaction:

$$k_1 = \alpha[\text{DO}], \quad k_2 = \beta(100 - [\text{DO}]), \quad (22)$$

where $\alpha, \beta =$ reaction coefficients(1/s), DO = saturation of DO(%).

The sorbed mass of Fe and Mn per unit mass of the sorbent is

$$\frac{C_p}{S} = \frac{(1 - f_d)C_t}{S}. \quad (23)$$

If the mass deposition rate of the suspended solids is F ($\text{mg}/(\text{cm}^2 \cdot \text{d})$), then the variation rate of concentration due to deposition for the i th layer of the water body is

$$r_d = \frac{(1 - f_d)C_t}{S} \frac{\Delta F_i}{\Delta z_i}. \quad (24)$$

where $\Delta F_i =$ net deposition rate of i th layer, $\Delta z_i =$ thickness of the i th layer.

The reactions and redox processes generate an *in situ* point source which may transport upwards to upper layers of the overlying water and downwards to the deeper sediment.

3 Flow fields

By cutting the water body into five layers, a grid is constructed whereby the resolution is $50\text{m} \times 50\text{m} \times 4.5\text{m}$. Open boundaries including the site of water intake are controlled by mean level of the flood season. Along a solid boundary, the normal components of the velocity and viscosity are set to zero. The velocities at surface and bottom layers are computed according to the corresponding shear stresses. Considering the thick sediment of similar texture at different parts of Arha Reservoir, a roughness of 0.02 is used in the whole reservoir. The wind drag coefficient is calculated by

$$C_a = \begin{cases} 0.0012875 & |w_{10}| < 7.5 \text{ m/s} \\ 0.0008 + 0.000065 |w_{10}| & |w_{10}| \geq 7.5 \text{ m/s} \end{cases}$$

Other parameters are calibrated to match the measured velocities (Table 2). Fig. 3 presents the average flow fields during summer on the top and bottom layers of the reservoir.

Table 2 Comparison of the simulated (S) and observed (O) velocities on top layer(cm/s)

Location No.	01		02		03		05		07		08	
	S	O	S	O	S	O	S	O	S	O	S	O
Magnitude	0.83	1.0	4.35	3.1	5.88	5.9	0.91	1.9	4.96	3.4	3.68	4.3
Direction	219	193	71	65	82	80	43	55	6	11	77	81

Note: for location No. see Fig. 1. Direction is degrees clockwise from the North

4 Suspended solids

The model (Equation(14)) was set up to simulate the average 3D distribution of suspended solids during flood season. The SS loads from the four tributaries were input as source terms. The traps were put at different water depth of 1m, 9m, and 19m in the upstream portion and the reservoir center simultaneously, measuring the mass deposition rate of the top, middle and bottom layers in Arha Reservoir. The average deposition rate of a 22 days survey were $4.11 \times 10^3 \text{ mg}/(\text{cm}^2$

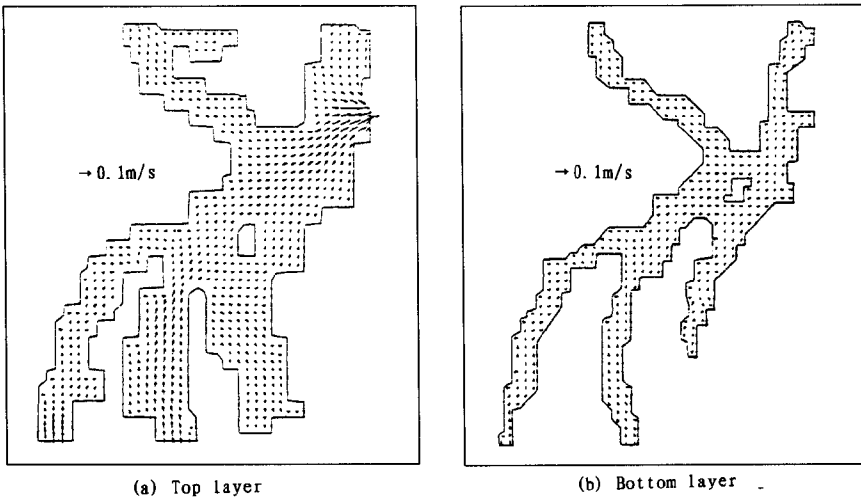


Fig.3 Flow fields on top and bottom layer

·d) in the top layer ($v_s = 0.82$ m/d), 2.92×10^3 mg/($\text{cm}^2 \cdot \text{d}$) in the middle layer ($v_s = 0.94$ m/d), and 3.6×10^2 mg/($\text{cm}^2 \cdot \text{d}$) in the bottom layer ($v_s = 4.81$ m/d). For the diffusion of SS in Arha Reservoir the turbulent diffusion has a principal role with $D_x = D_y = D_z = 80$ m^2/s . Comparison of the simulated and observed SS in water column is shown in Fig.4.

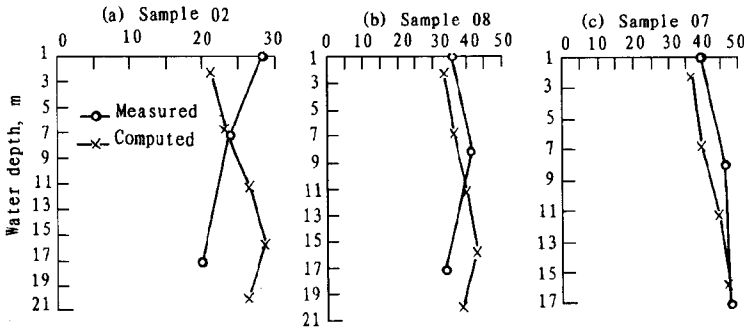


Fig.4 Comparison of simulated and observed SS

5 Exchange between water-column and sediment

The thickness of the sediment in Arha Reservoir is over 80 cm. It decreases from the entrance of Youyu River towards the reservoir center showing that sediments mainly come from Youyu River. There is a 10 cm suspension layer at the sediment surface which is rich in Fe and Mn (e.g. in the reservoir center, Fe: 12% and Mn: 2% at the beginning of the summer) and is the main source for Fe and Mn transport in the reservoir. Sediment profiles of Fe and Mn illustrate that the upper-8-cm-layer of the sediment is active for Fe and Mn reactions.

The analysis of the sediment samples from the entrance of Youyu River and the reservoir center showed that the average horizontal transport velocity of the sediments is 0.31 m/d.

The resuspension rate was found to be a relatively stable parameter with a value of about $5 \times$

10^{-8} (1/s). The adsorption/desorption coefficient plays a relatively small part in Fe and Mn exchange because adsorption and desorption are the reciprocal processes, and values of 9×10^{-6} /s for Fe and 3×10^{-5} /s for Mn were selected.

The modelled sediment layer, with a thickness of 10 cm, has a dry densities of 168.73 kg/m³. The solids mass in the sediment is assumed to be constant. It is also assumed that the partition coefficients in the water column and sediment are equal. The input coefficient of particles from surface sediment into permanent layer is estimated to be 5.2×10^{-6} (1/s). It was found that the reaction coefficient of reduction (β in Equation(22)) is the most sensitive parameter, and greatly influences the variation of total concentrations of Fe and Mn in both the water column and sediment. This shows that the soluble reduced forms of Fe and Mn play a principle role in transport processes within the sediment where particles are relatively immobile. During summer, DO in Arha Reservoir has a stable stratification (Fig.2) with the lowest saturation of DO of 26%—33% near the water sediment interface where the reduction mainly occurs. Fe and Mn are released to the overlying water resulting in high gradients of concentration in the lower layers of the reservoir. The gradients of Mn are much greater than that of Fe because Mn has a slower of oxidation and Mn is preferentially released from the sediment. Therefore, the reaction coefficient of oxidation (α in Equation(22)) for Mn is smaller than for Fe, while the reaction coefficient of reduction for Mn is larger than for Fe. The leaching experiments for Fe and Mn in sediment (sample location No.5 in Fig.1) under pH of 6 and 8 gave the leaching ratio of Fe: 2×10^{-5} — 6.2×10^{-5} , Mn: 1.7×10^{-4} — 11×10^{-4} . This illustrates the preferential release of Mn. The calibrated reaction coefficients are $\alpha(\text{Fe}) = 5 \times 10^{-8}$ (1/s), $\alpha(\text{Mn}) = 10^{-8}$ (1/s), $\beta(\text{Fe}) = 5 \times 10^{-9}$ (1/s), $\beta(\text{Mn}) = 10^{-7}$ (1/s).

Fe and Mn concentrations at the beginning of summer were input as initial conditions of the sediment model. The phenomenon in which the total concentrations of Fe and Mn in the sediment decrease during summer has been observed, for example at the reservoir center, where Fe and Mn fall from 12% and 2% respectively at the beginning of the summer to 5% and 0.2% respectively in early autumn. This is the result of the exchange by reduction, adsorption/desorption, desorption and resuspension of the particulate Fe and Mn in the sediment to the overlying water. Comparison of simulated and observed total concentrations of Fe and Mn in the sediment (simulated values were

Table 3 Simulated and observed total Fe and Mn concentrations in top layer of the sediment

Sample location No.	Fe, mg/kg		Mn, mg/kg	
	Observed	Simulated	Observed	Simulated
01	53000	49800	1900	2060
03	105000	103200	13300	12980
05	68000	60300	4500	4910
07	240000	237900	20000	19730
08	42000	51100	5700	5250

Note: the observed values were sampled on 27—28 Sep., 1993.

Simulated values are the average concentration for the summer

transformed into mg/kg by the dry density of the sediment) is shown in Table 3.

The redox boundary moves with the anoxia state though in Arha Reservoir the stratification of DO is relatively stable and the redox boundary stays at the water sediment interface most of the time during summer. The redox processes with a moving redox

boundary are very complex and were left for implementation at a later stage of the research.

6 Distributions of total Fe and Mn in water column

Coupled with the hydrodynamic model (Equation (1)—(10)) and the sediment model (Equation(13)) and the suspended solids model(Equation(14)), Equation(12) is used to simulate

the average distributions of total Fe and Mn in the water column during summer. The seasonal averaged Fe and Mn loads from the four tributaries were input as source terms. The comprehensive diffusion coefficients were determined to be $E_x = E_y = 460 \text{ m}^2/\text{s}$ and $E_z = 18 \text{ m}^2/\text{s}$. The exchange between the water column and the sediment is an in situ source of Fe and Mn which transport towards both upper water layers and deeper sediment.

The comparison of modeled and measured distributions of total concentrations of Fe and Mn in the water column of Arha Reservoir are shown in Fig. 5.

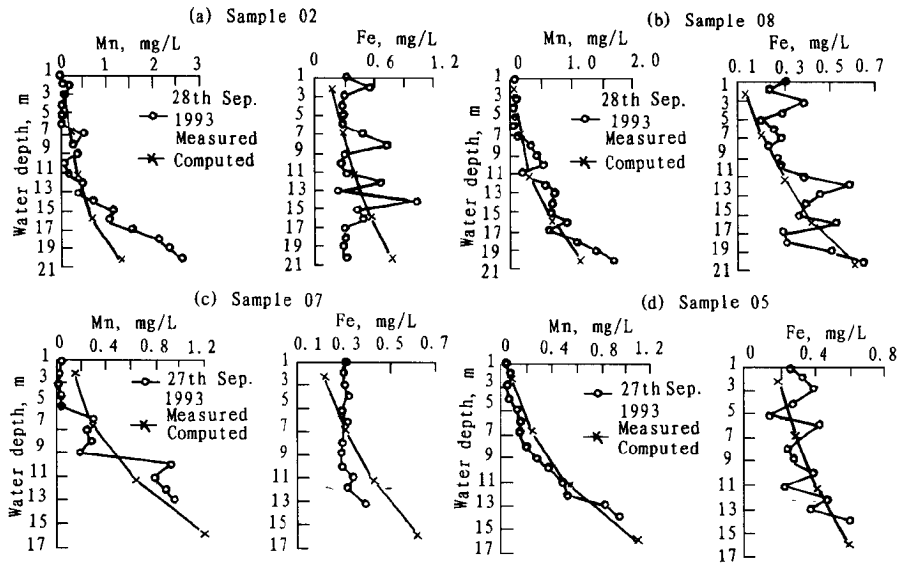


Fig.5 Comparison of modelled and measured distributions of Fe and Mn

Part of the simulated distributions of total concentrations of Fe and Mn in the water column are shown in Fig. 6 and 7. The results demonstrated that the distributions of Fe and Mn in the reservoir are unitary except for the four entrances and the near fields where the concentrations of Fe and Mn are larger due to the incoming larger Fe and Mn loads. It was found that Fe and especially Mn stratify in accordance with the stratification of DO during summer. The concentrations of Fe and Mn in the lower layers are larger than the upper layers and the largest concentration occurs in the reservoir bottom. In the horizontal directions, the transport rate of the Fe and Mn loads from the tributaries was found to be slow. The reaches of inflowing rivers are the main locations where the concentrations of Fe and Mn were influenced by the simultaneous Fe and Mn loads. For example, the Fe concentration at the entrance of Youyu River is 1.55 mg/L and decreases to 0.6 mg/L in the surface layer for the 400m length of river reach. The Fe and Mn bearing sediments move slowly towards the site of the water intake by the hydrodynamic action and most deposit to the reservoir bottom resulting in the rise of the concentrations of Fe and Mn in the sediment. Fe and Mn in the sediment are released back to the overlying water by reduction, resuspension, and desorption especially during anoxia in summer. The input loads from the four tributaries have a carryover effect on the water quality through a secondary contamination in the reservoir.

The oxido-reduction cycling on the sediment water interface for both Fe and Mn was found to be an important mechanism for the seasonal concentration rise. The sediment attributes most of the Fe and Mn concentrations in the lower layers of the reservoir during summer. The resuspension of

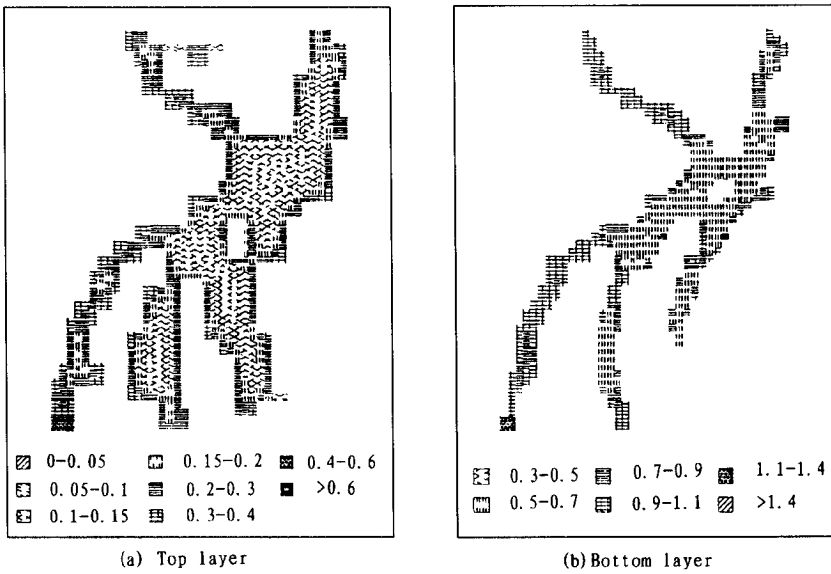


Fig.6 Simulated distributions of total Fe in the water column

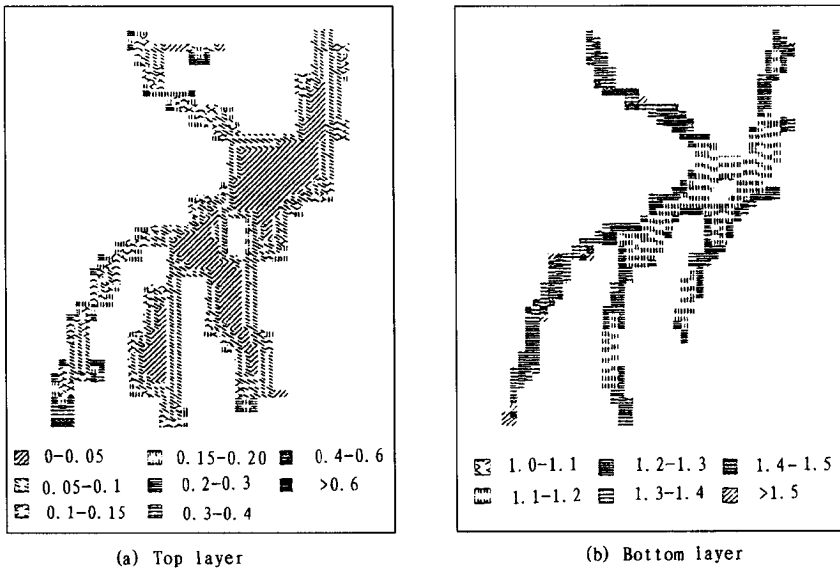


Fig.7 Simulated distributions of total Mn in the water column

the particles at the sediment surface promotes the release of Fe and Mn in pore water and results in the rise of concentration in the overlying water.

7 Conclusions

Fe and Mn transport in Arha Reservoir is complicated due to the complex topography and the many processes causing variation. The coupled 3D models of hydrodynamics and transportation of Fe and Mn in Arha Reservoir, developed in this paper, include the process of advection, diffusion,

redox, adsorption/desorption, deposition, and resuspension. The models showed good ability of modelling the distributions of Fe and Mn in the reservoir.

Both the measured samples and the estimated results showed that there are both horizontal and vertical gradients of Fe and Mn concentrations in Arha Reservoir and that the vertical gradients are more significant. It was found that Fe and Mn stratify correspondingly with the stratification of DO during summer. Mn has a slower oxidation rate and is released preferentially with a larger vertical concentration gradient in the bottom of the reservoir than for Fe. The redox cycles across the sediment-water interface was found to have a major role in the rise of Fe and Mn concentrations in the overlying water, especially during summer when the lower layers are in anoxia. The loads of Fe and Mn from the tributaries do not directly influence the simultaneous Fe and Mn concentrations in the reservoir except for the water fields near the tributary entrances. These loads have a carryover effect on the water quality through a secondary contamination in the reservoir, that is, Fe and Mn bearing sediments from the tributaries move slowly towards the site of water intake and most deposit to the reservoir bottom forming the source of Fe and Mn in the reservoir and result in the re-contamination of the overlying water.

References:

- Burdige D J, Gieskes J M, 1983. *Am J Sci*[J], 283:25—36.
- Calvert S E, Price N B, 1972. *Earth Planet Sci Lett*[J], 16:240—251.
- Chen X H, Brimicombe A J, 1997. *Water Pollution IV: modelling, measuring and prediction*[M](Ed. by R Rajar, C A Brebbia). Computational Mechanics Publications. 95—104.
- Coffey B M, Gallagher D L, Knocke W R, 1993. *J Environ Engrg ASCE*[J], 119(4): 679—694.
- Davison W, 1981. *Nature*[J], 290:241.
- Davison W, 1982. *Hydrobiologia*[J], 92: 456—468.
- Davison W, 1985. *Chemical processes in lakes*[M](Ed. by W Stumm). John Wiley & Sons. 31—53.
- Dortch M S, Hamlin-Tillman D E, 1995. *J Environ Engrg, ASCE*[J], 121(4):287—297.
- Elderfield H, 1976. *Marine Chem*[J], 4:98—107.
- Foster I D L, Charlesworth S M, 1996. *Hydrological Processes*[J], 10:227—261.
- Gordon J A, 1989. *Wat Resour Bull*[J], 1:187—192.
- Hess G W, Kim B R, Roberts P J W, 1989. *Wat Resour Bull*[J], 25(2):359—365.
- Hoffman M R, Eisenreich S J, 1981. *Enviorn Sci Technol*[J], 15:333—348.
- Imboden D M, Schwarzenbach R P, 1985. *Chemical processes in lakes*[M](Ed. by W Stumm). John Wiley & Sons. 1—30.
- Michrd G, 1971. *J Geophys Res*[J], 76:2175—2186.
- Morgan J J, 1967. *Principles and applications of water chemistry*[M](Ed. by Faust S U, Hunter J V). New York: Wiley. 561—624.
- Morgan J J and Stumm W, 1964. *Proceedings of the second international water pollution conference*[C], Tokyo. 100—109.
- Pankow J F, Morgan J J, 1981. *Enviorn Sci Technol*[J], 15:1155.
- Robbins J A, Callender E, 1975. *Am J Sci*[J], 275:509—520.
- Shrestha P L, Orlob G T, 1996. *J Envir Engrg, ASCE*[J], 122(8):730—739.
- Stumm W, 1985. *Chemical processes in lakes*[M]. John Wiley & Sons.31—55.
- Stumm W, 1987. *Aquatic surface chemistry: Chemical processes at the particle-water interface*[M]. John Wiley & Sons.18—42.
- Sung W, Morgan J J, 1980. *Environ Sci Technol*[J], 14:561.